Development of multicomponent-multiphase materials based on (Ti, Ta, Nb)C_xN_{1-x} carbonitride solid solutions

By José M. Córdoba*, E. Chicardi and Francisco J. Gotor

Instituto de Ciencia de Materiales de Sevilla, Centro Mixto CSIC-US, Américo Vespucio 49, 41092 Sevilla, Spain.

Abstract

A set of powdered cermets based on (Ti, Ta, Nb)C_xN_{1-x} carbonitride solid solutions were synthesized from mixtures of elemental powders by a mechanically induced self-sustaining reaction (MSR) method and subsequently sintered using a pressureless method. Differing nominal compositions of the hard phase were used, and the nature of the metallic-binder phase (Co, Ni, or Co-Ni) was varied. For comparative purposes, the design of the material was performed using two different synthesis pathways. The composition and microstructure of the ceramic and binder phases before and after sintering were analyzed and related to the microhardness of the material, which was found to increase with increasing contiguity of the hard phase and with decreasing particle size. The samples synthesized in one step (SERIES 2) showed higher microhardness and a more homogeneous microstructure with smaller particle size of the hard phase due to the presence of Ti, Ta, and Nb in the molten binder that hindered the ceramic growth during the liquid phase sintering.

Keywords: solid state reaction, mechanical milling, microstructure, ceramic matrix composite, processing

*Corresponding Author. E-mail: jmcordoba@icmse.csic.es, Phone: +34 954 489217

Introduction

Because of a highly desirable combination of properties, titanium carbonitride, along with other metal carbides and metallic binders, are used in cutting tools. However, they may not be used for heavy turning and interrupt milling equipment due to their relatively low toughness and low thermal shock resistance. For high-speed cutting applications, high temperature behavior is critical and more important than other mechanical properties such as toughness and mechanical shock resistance.

Modern cermets are traditionally made of a Ti(C,N) solid solution or mixtures of TiN and TiC as the primary hard component with Co/Ni as the binder. A variety of carbides such as Mo_2C, WC, TaC/NbC, etc. are added to improve the sinterability, hot hardness and thermal shock resistance. The addition of tantalum[1,2] (or the less expensive niobium[3]) increases the bending strength due to the formation of a high-strength complex carbonitride phase and has a positive effect on the material's resistance to plastic deformation. These systems exhibit highly complex behavior in their microstructure according to the type of additive used; therefore, great effort has been taken to improve the mechanical properties that are closely related to the microstructure developed during sintering.

Conventional methods of powder metallurgy do not allow for the production of some continuous single-phase carbonitrides from their carbides and nitrides[4]. As a promising alternative to the conventional methods, mechanically induced self-sustaining reactions (MSRs) have been employed to produce a variety of advanced materials including borides, carbides, nitrides, sulfides, hydrides, silicides, carbonitrides,

intermetallics, etc.[5-10] Although the preparation of the carbides [11-15] and nitrides[16,17] of transition metals (especially those in groups IVB and VB) by MSR has been investigated, research is comparatively lacking on the direct formation of the carbonitrides of transition metals through combustion synthesis and has focused largely on the synthesis of titanium carbonitrides[18]. In addition to Ti(C,N), Córdoba and coworkers[6,8,9] recently conducted a SERIESs of experimental studies on the formation of Nb, Ta, Hf, (Ti, Nb), (Ti, Ta), (Ti, Zr), (Ti, V) and (Ti, Hf) carbonitrides by MSR using a powder mixture of metals and graphite under a nitrogen atmosphere.

From a technical standpoint, if one desires to develop a new family of cermets using pre-made complex carbonitrides instead of unalloyed mixtures as the raw material to achieve a high level of quality and reliability, one must realize that the methods necessary to appropriately synthesize this new family of cermets have yet to be developed. MSR can then be considered as an alternative technique for use in the synthesis of complex carbonitride phases. The possibility of employing these complex phases allows for the development of new ways to optimize the set of properties that are targeted for specific technological applications.

Based on the above considerations, we put forward an innovative idea for development of a new family of (Ti, Ta, Nb)C_xN_{1-x}-based cermets. This work employs MSR as an alternative procedure for the fabrication of these materials in a simple, direct and effective way. We have evaluated the microstructural characteristics of the sintered material and focused on the changes in the chemical composition of the hard and binder phases during liquid phase sintering. We have attempted to find a relationship between

the raw powder characteristics and the microstructure and microhardness of the final cermets.

Materials and Methods

Titanium (99% pure, <325 mesh, Strem Chemicals), niobium (99.6% pure, <325 mesh, Strem Chemicals), tantalum (99.9% pure, <325 mesh, Aldrich), cobalt (99.8% pure, Strem Chemicals), nickel (puriss., Fluka), graphite (11 m^2/g, Fe≤0.4%, Merck) and high-purity N_2 gas (H_2O and O_2 ≤3 ppm, Air Liquide) were used in this work.

Powder mixtures with differing elemental molar ratios were ball milled under 6 bars of highly pure nitrogen gas using a modified planetary ball mill (model Micro Mill Puverisette 7, Fritsch) operating at a constant gas pressure and allowing for the detection of self-propagating reactions during milling[5]. Seven tempered steel balls, together with 6 g of powder, were placed in a tempered steel vial (67Rc) for each milling experiment and milled at 600 rpm. The volume of the vial was 50 cc. The diameter and mass of the balls were 15 mm and 13.41 g, respectively. The powder-to-ball mass ratio (PBR) was 1/15.65.

Cermets were fabricated through a pressureless process. Powdered cermets were first shaped (green bodies) and then sintered at high temperature to obtain hard cermets. The formation process was performed by means of cold isostatic pressing at 200 MPa for 5 min to yield cylinders of 12 mm in diameter and 45 mm in height. The green bodies were sintered at 1550 ºC for 60 min (heating rate = 10 ºC/min, free cooling) under an inert atmosphere (helium gas, H_2O≤3 ppm, O_2 ≤2 ppm and C_nH_m ≤0.5 ppm, Air Liquide)

in a horizontal furnace (AGNI GmbH). The sintering temperature was optimized in previous research [19]. The bulk densities of the cermets were measured by the water immersion technique (the Archimedes method).

X-ray diffraction diagrams of powders and polished surfaces of cermets were obtained with a Panalytical X'Pert Pro instrument equipped with a θ/θ goniometer using Cu K_α radiation (40 kV, 40 mA), a secondary K_β filter and an X'Celerator detector. The diffraction patterns were scanned from 30º to 80º (2θ) at a scanning rate of 0.42º min^{-1}. The lattice parameters were calculated from the entire set of peaks from the XRD diagram using the Fullprof[20] computer program assuming a suitable symmetry for all observed phases.

Scanning electron microscopy (SEM) and energy-dispersive X-ray (EDX) analysis were performed with a Hitachi FEG S-4800 microscope. The cermets were sectioned and polished until they acquired a mirror effect for the microhardness measurements and SEM observation. For reliable comparisons, the specimens were taken from the central part of each cermet. The Vickers test was performed at room temperature in a Microhardness FM-700 (Future-Tech. Corp) with a load of 9.81 N (Hv 1.0) for 15 s. Twelve micro-indentations were taken at different locations on the polished cermet, and the reported value was found from the average of the measured values.

Microstructural parameters were obtained from boundary intercepts with test lines on planar sections. The average number of intercepts per unit of length for the ceramic/binder interfaces, $(N_L)_{ceramic/binder}$, and for the ceramic/ceramic grain boundaries, $(N_L)_{ceramic/ceramic}$, was determined. From both parameters, the contiguity of the ceramic phase was calculated as follows:

$$C = 2(N_L)_{ceramic/ceramic} / [2(N_L)_{ceramic/ceramic} + (N_L)_{ceramic/binder}]$$

and the mean free path in the binder phase:

$$\lambda = \emptyset_{ceramic} / (N_L)_{ceramic/binder}$$

in which $\emptyset_{ceramic}$ is the mean particle size obtained from the particle-size distribution study.

Results and Discussion

1. Powdered cermets synthesis

Powdered cermets were prepared by MSR in a nitrogen atmosphere starting from elemental powders: titanium, niobium, tantalum, and graphite (necessary for (Ti, Nb, Ta)C_xN_{1-x} formation) with nickel and/or cobalt as the binder phase. The intended starting mixtures are shown in Table I. Additionally, three samples consisting of only a ceramic phase (without a metallic binder) were obtained from titanium, niobium, tantalum, and graphite mixtures (Table I). A combustion process took place in each mixture and the ignition times are also shown in the table. Milling was prolonged several minutes after combustion to obtain a homogeneous final product.

It is empirically suggested that MSR and SHS (self-propagating high-temperature synthesis) processes do not occur unless the adiabatic temperature is higher than 1800 K[21]. The adiabatic temperature, which measures the capacity for the self-heating of a mixture, represents the maximum temperature reached by a product resulting from an exothermic reaction and can be used to determine if a specific reaction proceeds via a

mechanically induced self-sustaining reaction. The adiabatic temperatures of **T8**, **T9**, and **T95** mixtures (ceramic phases) were determined using the protocol developed by Córdoba et al.[6] from the adiabatic temperature of the extreme binary compounds defining each quinary solid solution system. The calculated values were 3862 K, 3959 K, and 4007 K for samples **T8**, **T9,** and **T95**, respectively. In each case, the adiabatic temperature was well above the limit of 1800 K, confirming the presence of an MSR process.

The XRD diagrams of samples **T8**, **T9,** and **T95** obtained by MSR (Fig. 1(a)) show the formation of complex carbonitride phases that can be defined as (Ti, Nb, Ta)C_xN_{1-x}. The XRD diagrams also exhibit the shift in the reflections typical of differences in the Ti/Nb/Ta ratios in the stoichiometry of the (Ti, Nb, Ta)C_xN_{1-x} solid solutions. The symmetry in the XRD reflections of the quinary phases suggests that carbonitride solid solutions were obtained in which Ti, Ta and Nb atoms occupy the (0, 0, 0) positions, and C and N atoms occupy the (1/2, 1/2, 1/2) positions of the NaCl-type crystal structure. In contrast, the large broadening of the XRD reflections indicates that solid solutions with a nanometric grain microstructure were obtained. Careful examination of the XRD diagrams in Fig. 1(a) indicated the existence of a secondary minor phase, marked with a symbol (♠) in Fig. 1, which can also be indexed as TaC_xN_{1-x} (see Table II) in the cubic system and Fm–3m space group. In addition, all of the samples indicated the presence of small amounts of unreacted metallic titanium, niobium, and/or tantalum.

Adding up to 20 wt% of binder (Co and/or Ni) that did not participate in the MSR process to the initial Ti/Nb/Ta/C mixture did not inhibit the formation of (Ti, Nb,

Ta)C_xN_{1-x} by a combustion reaction. Rather, the addition caused an increase in the ignition time by ~10 min due to the presence of the binder phases, which were considered inert with regards to the Ti/Nb/Ta/C mixture (Table I). In particular, ductile nickel and/or cobalt can absorb part of the energy imparted by the mill through ball–ball and ball–wall impacts. Not all of the energy transmitted by the milling device was transferred to the reactive Ti/Nb/Ta/C mixture, and, consequently, the ignition was delayed.

Nickel and cobalt were inert with regards to the MSR (Ti, Nb, Ta)C_xN_{1-x} synthesis, however, the simultaneous reaction of Ni and/or Co with Ti, Ta, and Nb extracting these elements from the starting mixture used to obtain the ceramic phase was also observed. This was evidenced by the presence of (Co, Ni)–(Ti,Ta,Nb) intermetallic phases in the powdered cermets (Figs. 1(b), 1(c) and 1(d)). These intermetallic phases were primarily observed with compositions of 1:1 and 2:1. The XRD reflections corresponding to the intermetallics were shifted from each other and from the standard ICSD phases, which are related to a change in the lattice parameter due to the formation of intermetallic solid solutions. In previous experiments, X-ray diffraction of powder mixtures of Ni and Ti milled under similar conditions did not show any interaction between the two metals[22] suggesting that the formation of intermetallic solid solution phases was triggered by the heat released during the combustion process involved in the carbonitride phase formation.

The lattice parameter for each carbonitride phase, calculated using the Fullprof software, is shown in Table II. When the amount of niobium and tantalum was increased, a higher value for the lattice parameter of the carbonitride phase was observed as a

consequence of a higher expansion of the titanium carbonitride lattice, which can be considered the host structure. Powdered cermets (samples containing Co, Ni or Ni/Co) showed larger lattice parameters than those of the corresponding ceramic samples (**T8**, **T9**, and **T95**). In the powdered cermets, titanium was preferably extracted by Co and/or Ni from the reactant mixture to form the intermetallic solid solutions and induced the formation of a carbonitride solid solution phase with higher niobium and tantalum contents leading to increased lattice parameters. Moreover, the lattice parameters of the complex carbonitride phases were larger when Ni was used as the binder. This finding indicated that nickel extracted more titanium than cobalt for the formation of the intermetallic solid solution phase.

EDX compositional surface mapping was performed on the powdered cermets to analyze the distribution of the elements involved in the MSR process, and a characteristic map corresponding to the **T9**Co sample is shown in Fig. 2. The presence of carbon and nitrogen in the ceramic particles and the effective dispersion of the titanium, niobium and tantalum are evidence of the formation of a complex carbonitride phase. It is worth noting that the binder phase (cobalt in this case) was also well distributed in the sample; a finding that is extremely important for the subsequent sintering processes.

2.- Powdered cermets sintering

Two SERIES of cermets were densified (Table III). The first one (SERIES 1: Tx+Binders) was obtained by sintering a powder mixture composed of samples **T8**, **T9,** or **T95** (complex carbonitrides obtained by MSR) and the metallic binder (Ni and/or Co),

which was added after the synthesis of the ceramic phase. The powder mixture was homogenized by manual milling in a mortar for 10 min. The second Series (SERIES 2: TxBinders) corresponds to cermets sintered from the powdered cermets in Table II, which were obtained by a one-step MSR process.

XRD diagrams of the consolidated cermets are shown in Fig. 3, in which the reflections for the complex carbonitride and the metallic-binder phases are observed. For both seriess, the binder phases were composed of intermetallics. In the case of SERIES 1, the binder phases were produced during the high-temperature sintering process. For SERIES 2, the intermetallics were already present in the powdered cermets and the high-temperature sintering process merely induced changes in the chemical composition of these intermetallics as suggested by a comparison of Figs. 1 and 3. Examination of the XRD reflections corresponding to the intermetallics again showed the existence of solid solutions with a basic structure formed by the lattices described as hexagonal Ni_3(Ti,Ta,Nb) (JCPDS: 05-0723), orthorhombic Ni_3(Nb, Ta, Ti) (JCPDS: 15-0101), cubic Co_2(Ti,Ta,Nb) (JCPDS: 17-0031), hexagonal Co_2(Ti,Ta,Nb) (JCPDS: 05-0719) and cubic Co(Ti,Ta,Nb) (JCPDS: 18-0429). Compositional fluctuations in the intermetallic solid solutions were observed among the different cermets. It is noteworthy that when the amount of niobium and tantalum was increased, the content of the intermetallic phase in the cermets also increased and an intermetallic phase poorer in Co or/and Ni was formed. By increasing the content of Nb and Ta, the reaction of formation of the carbonitride phase becomes less exothermic, and possibly full conversion was not achieved remaining a greater amount of free Ti, Ta, and Nb to form the intermetallic phase.

The lattice parameters for the complex carbonitrides in all of the cermets are presented in Table III. A preliminary description of the nature of the binder phases, as observed by XRD, is also shown. Two tendencies were observed in comparing the results from Tables II and III (Fig. 4). In SERIES 1, the complex carbonitride phase had a larger lattice parameter after sintering. However, in SERIES 2, the resulting complex carbonitride had a slightly smaller lattice parameter after sintering. These changes in the complex carbonitride stoichiometry, as reflected by variations in the lattice parameter, cannot be explained in terms of the varying thermodynamic stability of carbon and nitrogen because transition metals have a similar affinity for carbon and nitrogen at high temperature, as shown by Kang et al.[23,24] The high temperature stability of transition metal carbonitrides was confirmed in a monolithic sample of titanium carbonitride, which, after processing at 1700 °C for 3 h under an inert atmosphere, did not show any compositional change.

The differing behaviors observed in the SERIES 1 and SERIES 2 cermets regarding changes in their lattice parameters (carbonitride stoichiometry) were related to differences in dissolution-reprecipitation processes involving the complex carbonitrides during sintering and were affected by the composition of the melted binder. The ceramic phase dissolution in the melted binder occurs through decomposition as its elemental constituents are incorporated into the liquid phase. Therefore, the stoichiometric changes observed in SERIES 1 samples (the increase in their lattice parameters) can be explained by taking into account the fact that the dissolution in the binder of the main ceramic phase and the minor phases observed after the MSR procedure, such as the unreacted metals and their subsequent incorporation into the complex carbonitride, occurred during

sintering. In the case of the SERIES 2 samples, the presence of the intermetallic phases prior to the sintering process reduced the dissolution of the ceramic phase in the binder, and only a small decrease in the lattice parameter was observed suggesting a composition slightly richer in Ti, probably induced by the preferential presence of this element in the intermetallic binder.

The selected SEM images showing the polished surface of the studied cermets are presented in Fig 5. The characteristic microstructural parameters of the cermets are listed in Table IV including the mean ceramic grain size, the binder mean free path, the ceramic contiguity, the phase volume fraction of the components and the porosity. Although the ceramic phase obtained by MSR has been previously proven to have nanometric characteristerics, the microstructure, as observed by SEM, did not show nanosized particles. This observation is not surprising because a sharp increase in grain growth at the micrometric level has frequently been observed during conventional sintering when densities close to the theoretical maximum are reached in systems with nanocrystalline particles[25].

The grain size was affected by the initial composition and the synthesis path. When the amounts of niobium and tantalum were increased in the initial mixture, smaller ceramic grains were observed, which suggested that ceramic growth was hindered by the presence of Nb and Ta in the host titanium carbonitride structure. In contrast, the SERIES 1 cermets generally showed coarser ceramic grain sizes than those in SERIES 2 (see Table IV and Fig. 6). The presence of a high quantity of transition metals (Ti, Ta, and Nb) in the melted binder in SERIES 2 should reduce the solubility of the ceramic particles during the liquid phase sintering and hinder growth by a solution-reprecipitation

process. In SERIES 1 cermets, the growth is enhanced by a binder free of Ti, Ta, and Nb, which favors the dissolution of the smaller ceramic particles and the reprecipitation on the larger ones, which thus continue to grow. Since the volume fraction of ceramic particles in the cermets is large, their growth can also induce a coalescence process that leads to the formation of even coarser particles [26]. A binder phase located inside large particles proved that they had grown by a coalescence process (Fig. 7). Evidence of such growth can be observed in the different regions of the SEM micrographs. The slightly smaller contiguity values for samples from SERIES 1, prepared by a two-step procedure, indicate that there was a more homogenous distribution of the ceramic grains in the binder phase than in SERIES 2, as is observed in Fig. 5.

The component phase volume fraction was determined by image analysis, as shown in Table IV. The volume fraction of the binder phase tended to be stable within a range of 23 to 36% in both series studied because of the similar weights of the metallic cobalt and/or nickel used as binders. Binder areas of varying contrast were found on the SEM micrographs (Fig. 7), and when they were analyzed by EDX (inset Fig. 7), slightly different compositions were observed indicating the formation of intermetallic solid solutions.

The microhardness of the cermets was evaluated and the results are shown in Table IV. The presence of cobalt in the intermetallic solid solutions caused hardening in the cermets due to a greater contribution to the hardness from Co (H_v=10.3 GPa) than from Ni (H_v=6.3 GPa). The influence of the nature of the binder on the Vickers microhardness of cermets is not evident from the results presented in Table IV. However, the microhardness of the studied cermets proved to be particularly sensitive to the

contiguity of the hard phase. In general, when samples containing the same type of binder (Co, Ni or CoNi/Co) are compared, the microhardness was found to increase with increasing contiguity of the hard phase and with decreasing particle size. A more compact complex carbonitride skeletal structure with increased rigidity was formed enhancing the hardness of the material. The overall comparison of the results independent of the cermet composition showed no clear dependence of the microhardness with the different studied factors (chemical composition and microstructural parameters) probably due to the variability in the binder phase composition.

Conclusions

Powdered cermets produced by MSR showed larger lattice parameters than did the corresponding ceramic samples (**T8**, **T9**, and **T95**). In the powdered cermets, titanium was preferably extracted by Co and/or Ni from the reactant mixture to form the intermetallic solid solutions inducing the formation of a carbonitride solid solution phase with a higher content of niobium and tantalum, which led to increasing lattice parameters.

Varying the composition of the melted binder used in the dissolution-reprecipitation processes during sintering produced changes in the lattice parameter. The presence of a large quantity of Ti, Nb, and Ta in the melted Co/Ni binder should reduce the solubility of ceramic particles hindering their growth by a solution–reprecipitation process.

The microhardness of cermets with the same type of binder proved to be particularly sensitive to contiguity of the hard phase. The rigidity of the material was

enhanced by the formation of a complex carbonitride three-dimensional network structure.

Acknowledgments

This work was supported by the Spanish government under grant No. MAT2010-17046, which is financed in part by the European Regional Development Fund of 2007–2013. E. Chicardi and J. M. Córdoba were supported by CSIC through JAE-Pre and JAE-Doc grants, respectively, which are financed, in part, by the European Social Fund (ESF).

References

[1] U. Rolander, G. Weinl, M. Zwinkels, Effect of Ta on structure and mechanical properties of (Ti,Ta,W)(C,N)-Co cermets, Int. J. Refract. Met. Hard Mater. 19 (2001) 325-328.

[2] V. I. Tret'yakov, V. L. Mashevskaya, Effect of tantalum on the properties and structure of hard alloys based on titanium carbonitride, Powd. Metal. Met. Ceram. 38 (1999) 64-67.

[3] F. Qi, S. Kang, A study on microstructural changes in Ti(CN)-NbC-Ni cermets, Mater. Sci. Eng. A, 251 (1998) 276-285.

[4] O. Y. Khyzhun, V. A. Kolyagin, Electronic structure of cubic and rhombohedral tantalum carbonitrides studied by XPS, XES, and XAS methods, J. Electron Spectrosc. Relat. Phenom. 137 (2004) 463-467

[5] M. A. Aviles, J. M. Córdoba, M. J. Sayagués, M. D. Alcala, F. J. Gotor, Mechanosynthesis of Hf1-xZrxB2 Solid Solution and $Hf_{1-x}Zr_xB_2$/SiC Composite Powders, J. Amer. Ceram. Soc. 93 (2010) 696-702.

[6] J. M. Córdoba, M. A. Aviles, M. J. Sayagués, M. D. Alcala, F. J. Gotor, Synthesis of complex carbonitride powders $Ti_yM_{T1-y}C_xN_{1-x}$ (M-T: Zr, V, Ta, Hf) via a mechanically induced self-sustaining reaction, J. Alloys Comp. 482 (2009) 349-355.

[7] J. M. Córdoba, R. Murillo, M. D. Alcala, M. J. Sayagués, F. J. Gotor, Synthesis of TiN/Si_3N_4 composite powders by mechanically activated annealing, J. Mater. Res. 20 (2005) 864-873.

[8] J. M. Córdoba, M. J. Sayagués, M. D. Alcala, F. J. Gotor, Monophasic $Ti_yNb_{1-y}C_xN_{1-x}$ nanopowders obtained at room temperature by MSR, J. Mater. Chem. 17 (2007) 650-653.

[9] J. M. Córdoba, M. J. Sayagués, M. D. Alcala, F. J. Gotor, Monophasic nanostructured powders of niobium, tantalum, and hafnium carbonitrides synthesized by a mechanically induced self-propagating reaction, J. Amer. Ceram. Soc. 90 (2007) 381-387.

[10] A. Bakhshai, V. Soika, M. A. Susol, L. Takacs, Mechanochemical reactions in the Sn-Zn-S system: Further studies, J. Solid State Chem. 153, (2000) 371-380.

[11] L. Takacs, Ball milling-induced combustion in powder mixtures containing titanium, zirconium, or hafnium, J. Solid State Chem. 125 (1996) 75-84.

[12] G. Lecaer, E. Bauergrosse, A. Pianelli, E. Bouzy, P. Matteazzi, Mechanically driven syntheses of carbides and silicides, J. Mater. Sci. 25 (1990) 4726-4731.

[13] Z. G. Liu, J. T. Guo, L. L. Ye, G. S. Li, Z. Q. Hu, Formation mechanism of TiC by mechanical alloying, App. Phys. Lett. 65 (1994) 2666-2668.

[14] Z. G. Liu, L. L. Ye, J. T. Guo, G. S. Li, Z. Q. Hu, Self-propagating high temperature synthesis of TiC and NbC by mechanical alloying, J. Mater. Res. 10 (1995) 3129-3135.

[15] P. Matteazzi, G. Lecaer, Room temperature mechanosynthesis of carbides by grinding of elemental powders, J. Amer. Ceram. Soc. 74 (1991) 1382-1390.

[16] U. K. Bhaskar, S. Bid, B. Satpati, S. K. Pradhan, Mechanosynthesis of nanocrystalline titanium nitride and its microstructure characterization, J. Alloys Comp. 493 (2010) 192-196.

[17] Z. H. Chin, T. P. Perng, In situ observation of combustion to form TiN during ball milling Ti in nitrogen, Appl. Phys. Lett. 70 (1997) 2380-2382.

[18] J. M. Córdoba, M. J. Sayagués, M. D. Alcala, F. J. Gotor, Synthesis of titanium carbonitride phases by reactive milling of the elemental mixed powders, J. Am. Ceram. Soc. 88 (2005) 1760-1764.

[19] E. Chicardi, J. M. Córdoba, and F. J. Gotor, Inverse core-rim microstructure in (Ti,Ta)(C,N)-based cermets developed by a mechanically induced self-sustaining reaction, Int. J. Refract. Metal. Hard. Mater. doi:10.1016/j.ijrmhm.2011.09.003.

[20] J. Rodríguez-Carvajal and R. Thiery, FullProf ILL May-2010.

21 Z. A. Munir, Synthesis of high temperature materials by self-propagating combustion methods, Amer. Ceram. Soc. Bull. 67 (1988) 342-349.

[22] J. M. Córdoba, M. D. Alcala, M. A. Aviles, M. J. Sayagués, F. J. Gotor, New production of TiC_xN_{1-x}-based cermets by one step mechanically induced self-sustaining reaction: Powder synthesis and pressureless sintering, J. Eur. Ceram. Soc. 28 (2008) 2085-2098.

[23] I. J. Jung, S. Kang, S. H. Jhi, J. Ihm, A study of the formation of Ti(CN) solid solutions, Acta Mater. 47 (1999) 3241-3245.

[24] S. Kang, Stability of N in Ti(CN) solid solutions for cermet applications, Powder Metal. 40 (1997) 139-142.

[25] R. S. Iyer, S. M. L. Sastry, Consolidation of nanoparticles - Development of a micromechanistic model, Acta Mater. 47 (1999) 3079-3098.

[26] G. Madras, B. J.. McCoy, Distribution kinetics of Ostwald ripening at large volume fraction and with coalescence, J. Colloid Interface Sci. 261 (2003) 423–433.

Figure Caption

Figure 1. X-ray powder diffraction diagrams of the products following the mechanically induced self-sustaining reaction process from the starting mixtures in Table I [# Ta, + Ti, │ Nb, ♠ TaC_xN_{1-x}, ○ Co(Ti,Ta,Nb), □ Ni(Ti,Ta,Nb), ♥ (Co,Ni)(Ti,Ta,Nb), © Co_2(Ti,Ta,Nb)].

Figure 2. EDX-SEM mapping of the T9Co powdered cermet showing the distribution of product components.

Figure 3. X-ray powder diffraction diagrams for SERIES 1 and SERIES 2 cermets after the sintering procedure from the starting mixtures in Table I [α, hexagonal Ni_3(Ti, Ta, Nb); β, orthorhombic Ni_3(Nb, Ta, Ti); χ, cubic Co_2(Ti, Ta, Nb), δ, cubic Co(Ti, Ta, Nb); λ, orthorhombic $(Co,Ni)_3$(Nb, Ta, Ti); μ, hexagonal Co_2(Ti, Ta, Nb)].

Figure 4. Comparison of carbonitride lattice parameter before and after sintering for (a) SERIES 1 and (b) SERIES 2.

Figure 5. Characteristic SEM micrographs of the T9+Cos, T95+Cos, T8Cos, T9Cos, T95Cos, T95+Nis, T9CoNis and T95+CoNis samples.

Figure 6. Particle size distribution of the ceramic phase in sintered cermets.

Figure 7. Characteristic SEM micrographs of cermets showing the binder phase inside the ceramic particle.

Table I. Summary of the starting elemental mixtures, milling times and ignition times for the samples studied.

Sample	Raw powders (atomic ratio) + binder (wt%)	t_{mol} (min)	t_{ig} (min)
T8	Ti/Ta/Nb/C (0.8/0.1/0.1/0.5)	50	43
T9	Ti/Ta/Nb/C (0.9/0.05/0.05/0.5)	50	43
T95	Ti/Ta/Nb/C (0.95/0.025/0.025/0.5)	50	43
T8Co	Ti/Ta/Nb/C (0.8/0.1/0.1/0.5) + 20% Co	60	52
T9Co	Ti/Ta/Nb/C (0.9/0.05/0.05/0.5) + 20% Co	60	52
T95 Co	Ti/Ta/Nb/C (0.95/0.025/0.025/0.5) + 20% Co	60	52
T8Ni	Ti/Ta/Nb/C (0.8/0.1/0.1/0.5) + 20% Ni	60	52
T9Ni	Ti/Ta/Nb/C (0.9/0.05/0.05/0.5) + 20% Ni	60	53
T95 Ni	Ti/Ta/Nb/C (0.95/0.025/0.025/0.5) + 20% Ni	60	53
T8CoNi	Ti/Ta/Nb/C (0.8/0.1/0.1/0.5) + 10% Co + 10% Ni	60	51
T9CoNi	Ti/Ta/Nb/C (0.9/0.05/0.05/0.5) + 10% Co + 10% Ni	60	55
T95 CoNi	Ti/Ta/Nb/C (0.95/0.025/0.025/0.5) + 10% Co + 10% Ni	60	52

Table II. Summary of phases found after milling and the lattice parameters for the ceramic phase.

Sample	Phases found after MSR process	a (Å)
T8	(Ti,Ta,Nb)(C,N), Ta, Nb, Ti, $TaC_{0.58}N_{0.42}$	4.3070(4)
T9	(Ti,Ta,Nb)(C,N), Ta, Nb, Ti, $TaC_{0.70}N_{0.30}$	4.2979(9)
T95	(Ti,Ta,Nb)(C,N), Ta, Nb, Ti, $TaC_{0.63}N_{0.37}$	4.2926(8)
T8Co	(Ti,Ta,Nb)(C,N), Ta, Nb, Ti, Co(Ti,Ta,Nb), Co_2(Ti,Ta,Nb)	4.3187(4)
T9Co	(Ti,Ta,Nb)(C,N), Ta, Nb, Ti, Co(Ti,Ta,Nb), Co_2(Ti,Ta,Nb)	4.3147(6)
T95 Co	(Ti,Ta,Nb)(C,N), Ta, Nb, Ti, Co(Ti,Ta,Nb), Co_2(Ti,Ta,Nb)	4.3137(6)
T8Ni	(Ti,Ta,Nb)(C,N), Ta, Nb, Ti, Ni(Ti,Ta,Nb)	4.3320(5)
T9Ni	(Ti,Ta,Nb)(C,N), Ta, Nb, Ti, Ni(Ti,Ta,Nb)	4.3229(7)
T95 Ni	(Ti,Ta,Nb)(C,N), Ta, Nb, Ti, Ni(Ti,Ta,Nb)	4.3164(7)
T8CoNi	(Ti,Ta,Nb)(C,N), Ta, Nb, Ti, (Co,Ni)(Ti,Ta,Nb)	4.3294(0)
T9CoNi	(Ti,Ta,Nb)(C,N), Ta, Nb, Ti, (Co,Ni)(Ti,Ta,Nb)	4.3183(4)
T95 CoNi	(Ti,Ta,Nb)(C,N), Ta, Nb, Ti, (Co,Ni)(Ti,Ta,Nb)	4.3150(4)

Table III. Summary of phases found after sintering for the two series cermets, the lattice parameters of the ceramic phase and the density measured by the Archimedes method.

Sample	Phases found after the sintering process	a (Å)	Density (g/cm^3)
SERIES 1			
T8+Cos	(Ti,Ta,Nb)(C,N), cubic [Co_2(Ti, Ta, Nb)]	4.3148(6)	6.48
T9+Cos	(Ti,Ta,Nb)(C,N), hexagonal [Co_2(Ti, Ta, Nb)]	4.3089(2)	5.80
T95+Cos	(Ti,Ta,Nb)(C,N), cubic [Co_2(Ti, Ta, Nb)]	4.3039(2)	5.81
T8+Nis	(Ti,Ta,Nb)(C,N), unknown	4.3248(0)	6.34
T9+Nis	(Ti,Ta,Nb)(C,N), orthorhombic [Ni_3(Nb,Ta,Ti)]	4.3106(4)	5.65
T95+Nis	(Ti,Ta,Nb)(C,N), hexagonal [Ni_3(Ti, Ta, Nb)]	4.3028(2)	5.21
T8+CoNis	(Ti,Ta,Nb)(C,N), orthorhombic [$(Ni,Co)_3$(Nb,Ta,Ti)]	4.3259(6)	6.29
T9+CoNis	(Ti,Ta,Nb)(C,N), orthorhombic [$(Ni,Co)_3$(Nb,Ta,Ti)]	4.3181(6)	5.74
T95+CoNis	(Ti,Ta,Nb)(C,N), orthorhombic [$(Ni,Co)_3$(Nb,Ta,Ti)]	4.3068(4)	5.57
SERIES 2			
T8Cos	(Ti,Ta,Nb)(C,N), cubic [Co_2(Ti, Ta, Nb)], cubic [Co(Ti, Ta, Nb)]	4.3217(2)	6.51
T9Cos	(Ti,Ta,Nb)(C,N), cubic [Co(Ti, Ta, Nb)]	4.3104(8)	5.90
T95 Cos	(Ti,Ta,Nb)(C,N), hexagonal [Co_2(Ti, Ta, Nb)]	4.3146(0)	5.68
T8Nis	(Ti,Ta,Nb)(C,N), hexagonal [Ni_3(Ti, Ta, Nb)]	4.3295(8)	6.25
T9Nis	(Ti,Ta,Nb)(C,N), orthorhombic [Ni_3(Nb,Ta,Ti)]	4.3160(0)	5.68
T95 Nis	(Ti,Ta,Nb)(C,N), orthorhombic [Ni_3(Nb,Ta,Ti)]	4.3036(6)	5.56
T8CoNis	(Ti,Ta,Nb)(C,N), orthorhombic [$(Ni,Co)_3$(Nb,Ta,Ti)]	4.3181(2)	6.63
T9CoNis	(Ti,Ta,Nb)(C,N), orthorhombic [$(Ni,Co)_3$(Nb,Ta,Ti)]	4.3070(0)	6.12
T95 CoNis	(Ti,Ta,Nb)(C,N), orthorhombic [$(Ni,Co)_3$(Nb,Ta,Ti)]	4.3049(0)	6.06

Table IV. Vickers hardness, contiguity and average free pathway, with the average ceramic particle size, ceramic volume, binder volume and porous volume that were extracted from the image analysis of the selected samples.

				Image Analysis			
Sample	H_v (1.0) GPa	Contiguity (C)	Mean free path (μm)	Ceramic Particle Size (μm)	Ceramic Volume (% vol)	Binder Volume (% vol)	Porous Volume (% vol)
SERIES 1							
T8+Cos	14.6	0.30	1.4	3.2	60	36	3
T9+Cos	12.4	0.23	1.0	2.7	67	32	1
T95+Cos	12.1	0.27	2.2	6.2	64	35	1
T8+Nis	11.7	0.31	1.0	2.9	65	31	4
T9+Nis	10.5	0.28	1.2	4.0	69	28	3
T95+Nis	10.7	0.26	1.6	5.6	72	25	3
T8+CoNis	12.2	0.39	0.5	2.0	70	29	1
T9+CoNis	11.4	0.31	0.8	3.2	73	26	1
T95+CoNis	12.5	0.35	0.8	3.3	72	27	1
SERIES 2							
T8Cos	12.1	0.32	0.9	3.0	68	30	2
T9Cos	11.0	0.25	1.7	3.9	61	36	3
T95 Cos	13.3	0.41	0.7	2.6	69	30	1
T8Nis	10.7	0.38	0.6	2.2	69	28	4
T9Nis	10.9	0.36	0.4	2.3	75	23	2
T95 Nis	11.0	0.35	0.8	3.0	71	27	2
T8CoNis	14.1	0.39	0.6	2.9	74	25	1
T9CoNis	13.9	0.37	0.7	3.2	73	26	1
T95 CoNis	12.7	0.34	1.0	4.0	71	28	1

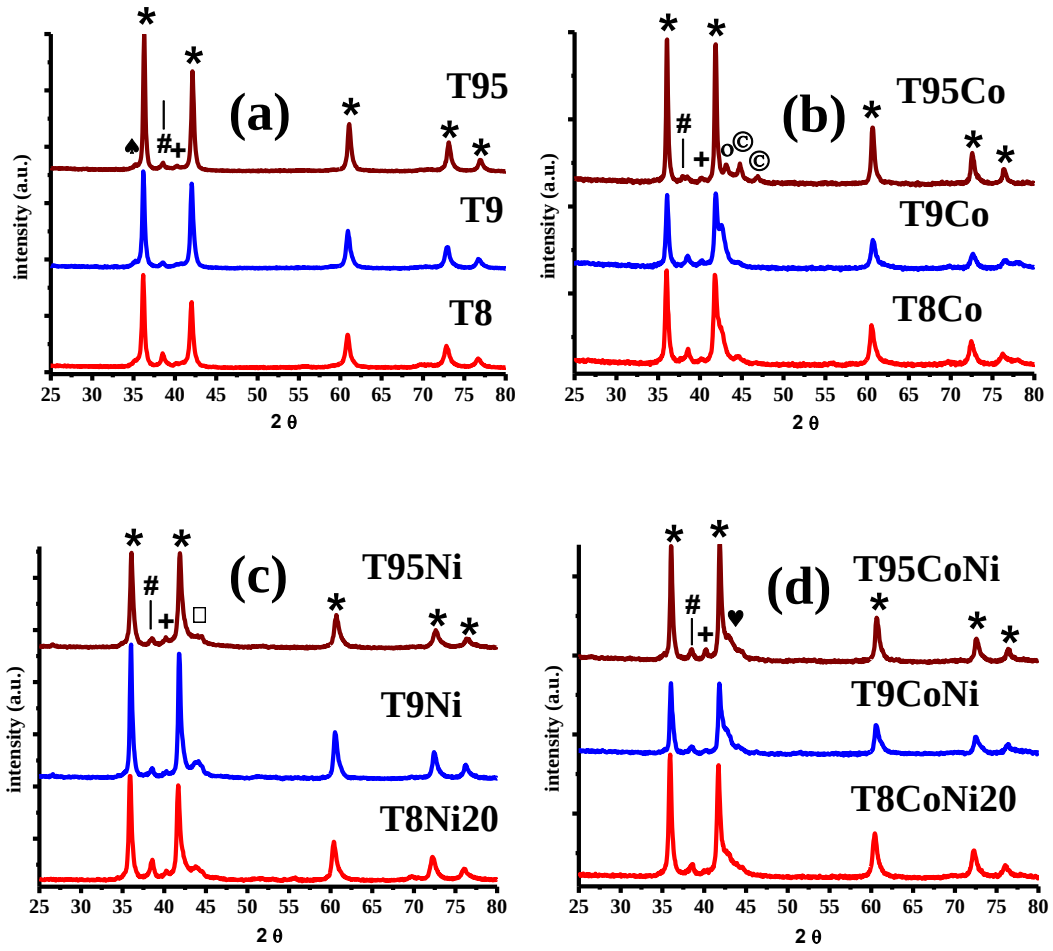
(a)
T95
T9
T8
intensity (a.u.)
2 θ
(b)
T95Co
T9Co
T8Co
intensity (a.u.)
2 θ
(c)
T95Ni
T9Ni
T8Ni20
intensity (a.u.)
2 θ
(d)
T95CoNi
T9CoNi
T8CoNi20
intensity (a.u.)
2 θ

Figure 1

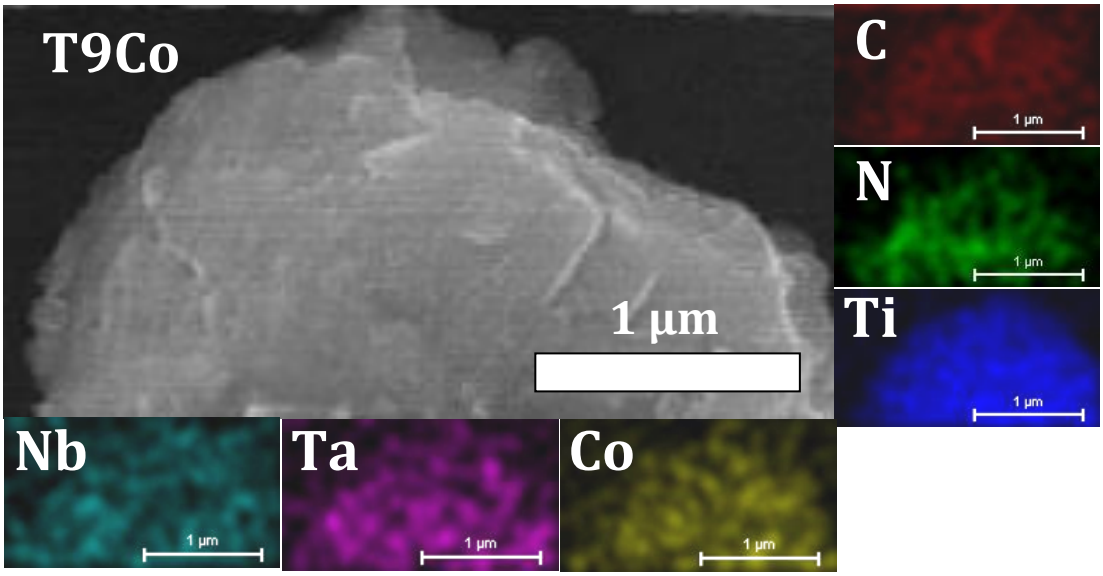

Figure 2

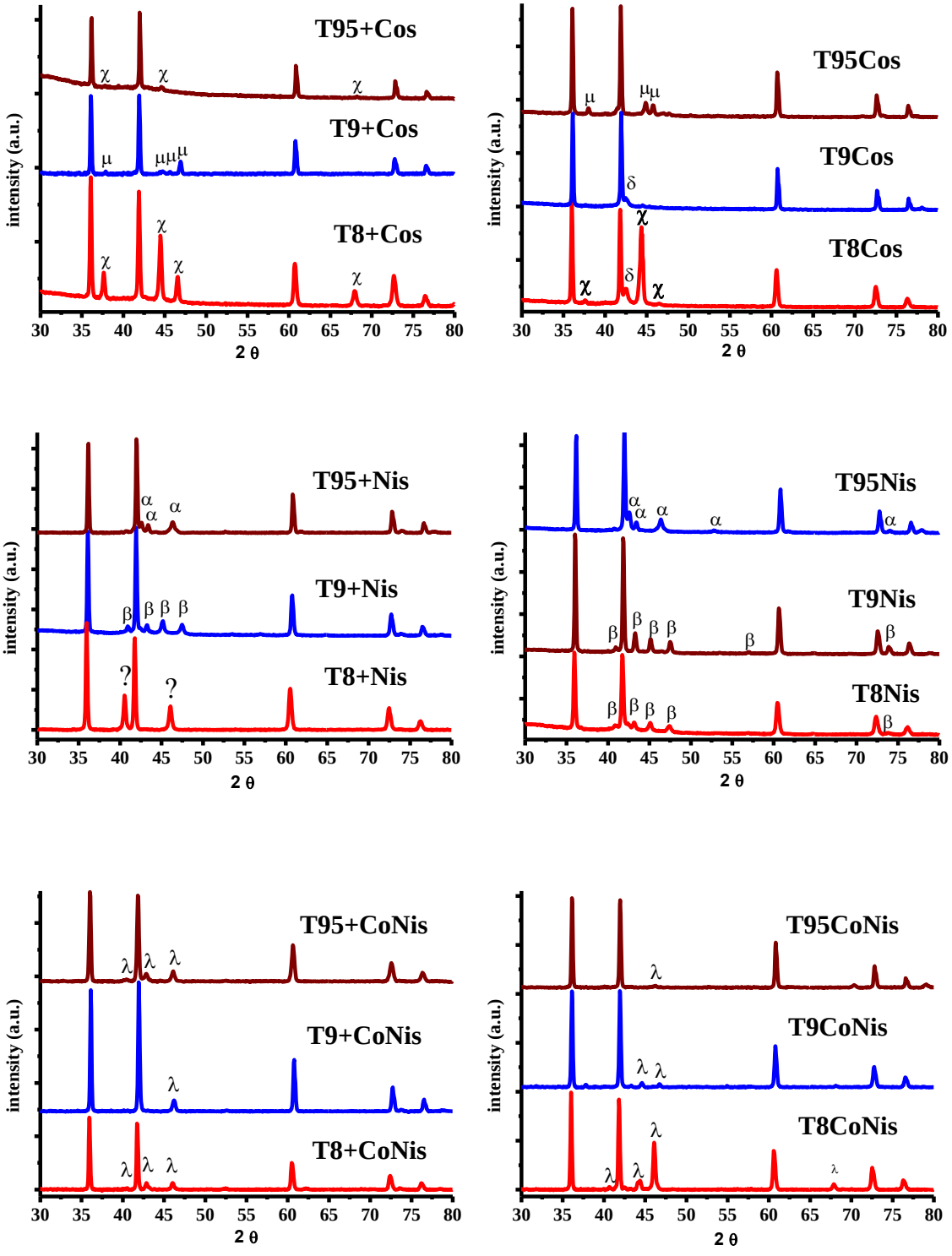
T95+Cos
T9+Cos
T8+Cos
T95Cos
T9Cos
T8Cos
T95+Nis
T9+Nis
T8+Nis
T95Nis
T9Nis
T8Nis
T95+CoNis
T9+CoNis
T8+CoNis
T95CoNis
T9CoNis
T8CoNis
intensity (a.u.)
2 θ

Figure 3

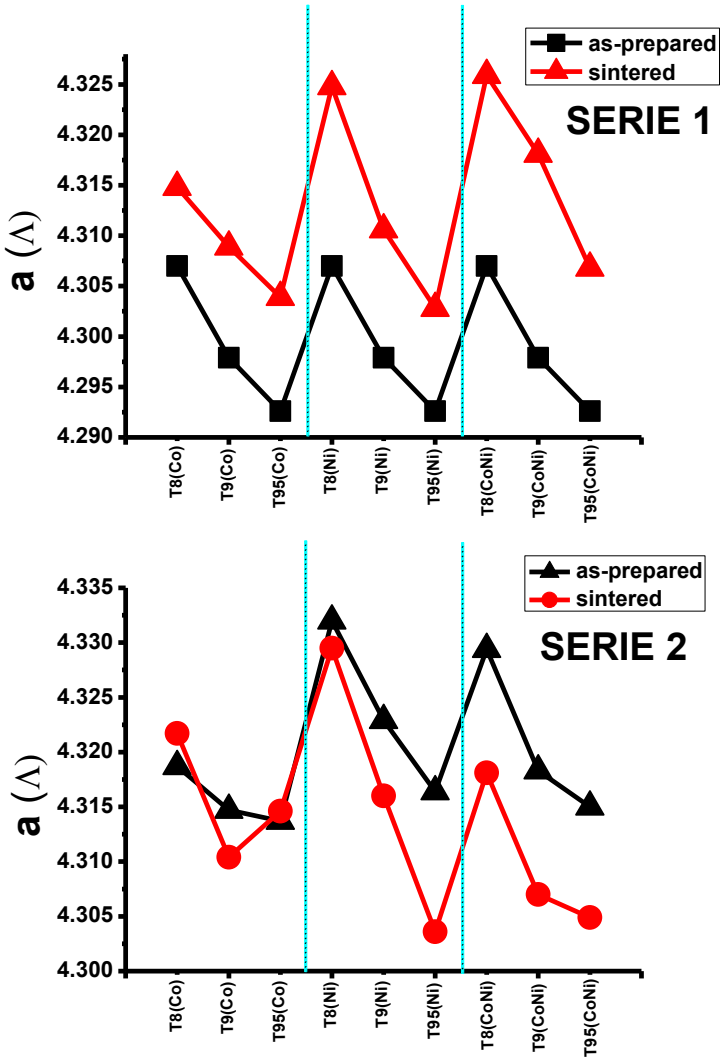
as-prepared
sintered
SERIE 1
a (Å)
4.325
4.320
4.315
4.310
4.305
4.300
4.295
4.290
T8(Co)
T9(Co)
T95(Co)
T8(Ni)
T9(Ni)
T95(Ni)
T8(CoNi)
T9(CoNi)
T95(CoNi)
as-prepared
sintered
SERIE 2
a (Å)
4.335
4.330
4.325
4.320
4.315
4.310
4.305
4.300
T8(Co)
T9(Co)
T95(Co)
T8(Ni)
T9(Ni)
T95(Ni)
T8(CoNi)
T9(CoNi)
T95(CoNi)

Figure 4

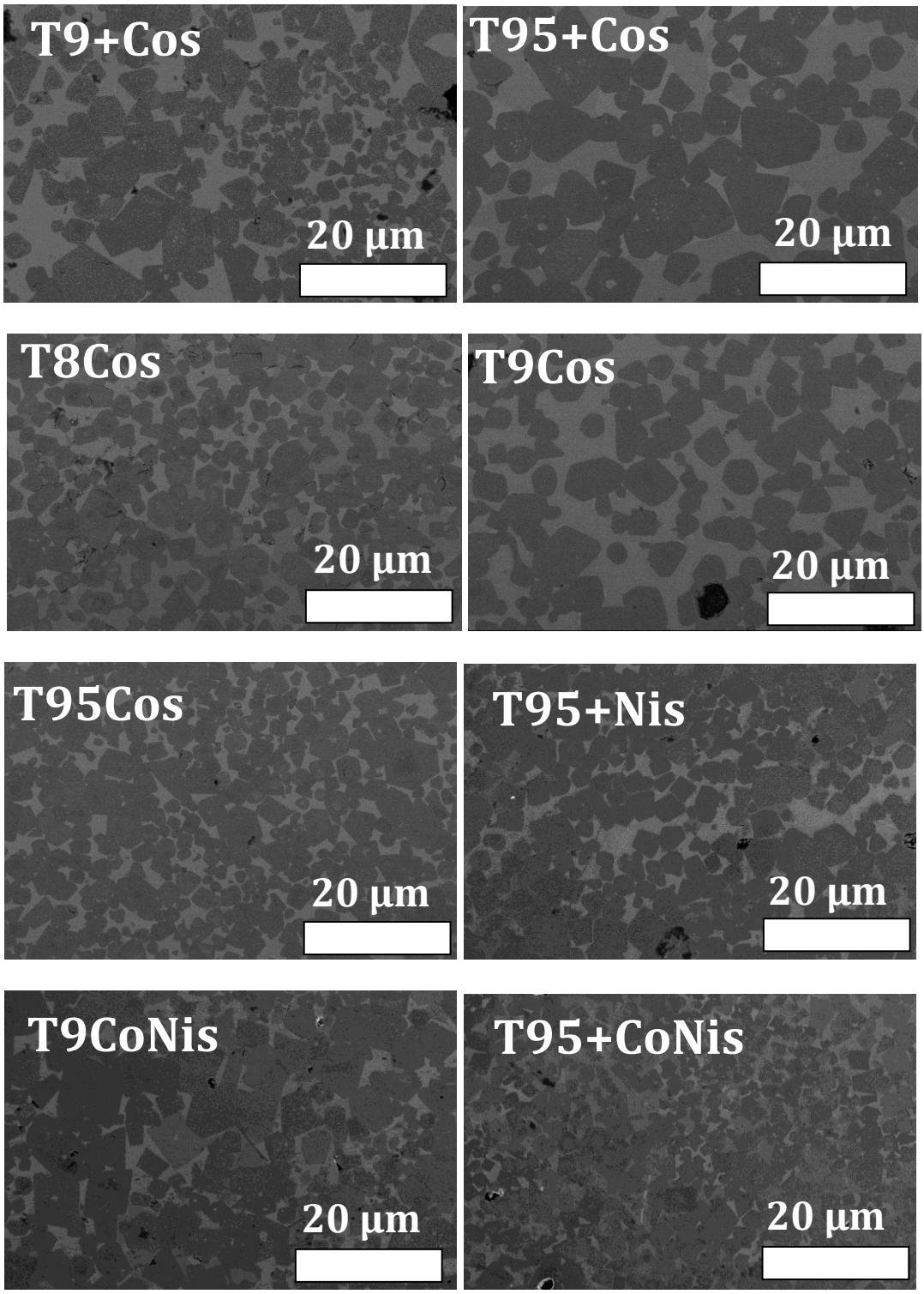
T9+Cos
20 µm
T95+Cos
20 µm
T8Cos
20 µm
T9Cos
20 µm
T95Cos
20 µm
T95+Nis
20 µm
T9CoNis
20 µm
T95+CoNis
20 µm

Figure 5

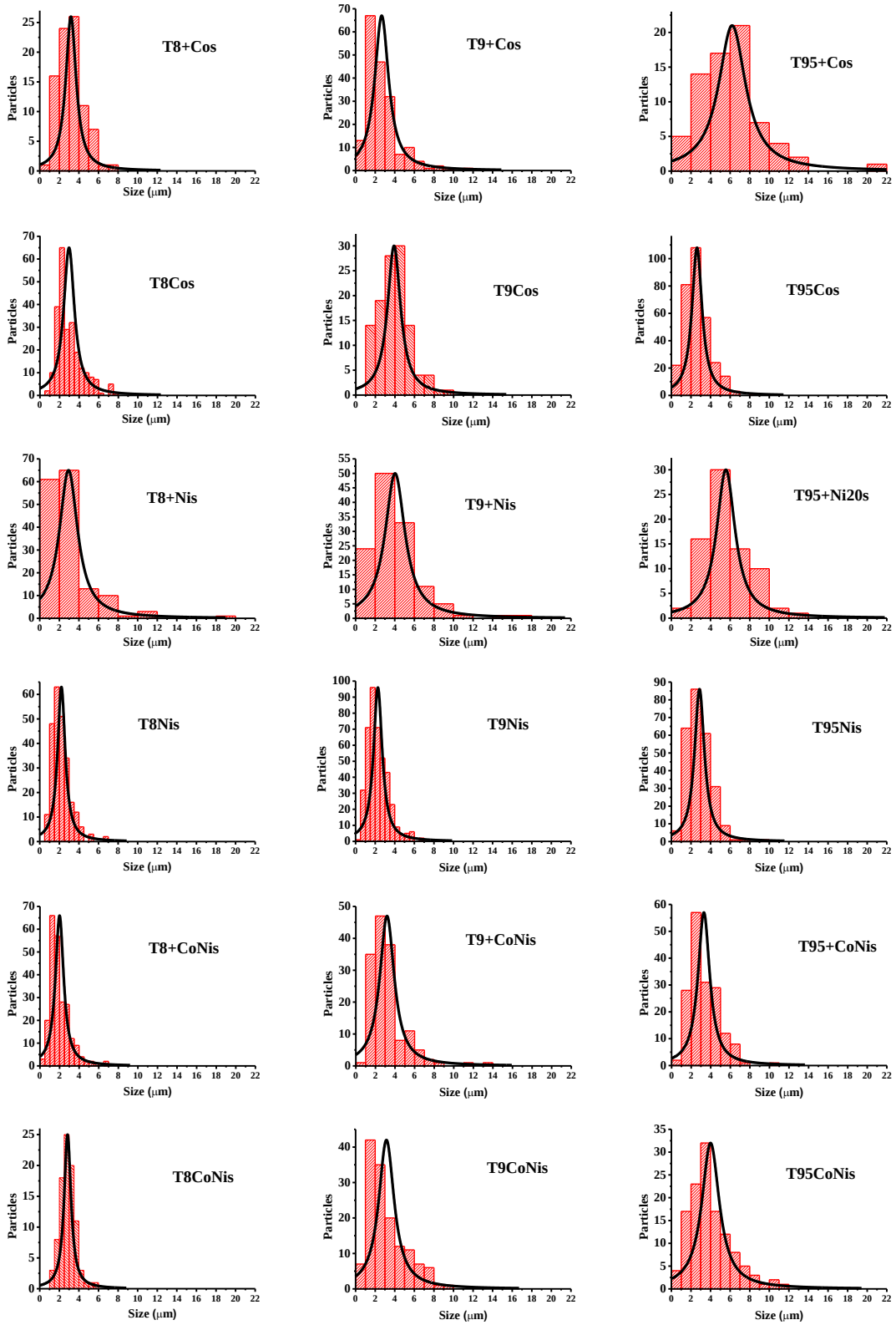
T8+Cos
T9+Cos
T95+Cos
T8Cos
T9Cos
T95Cos
T8+Nis
T9+Nis
T95+Ni20s
T8Nis
T9Nis
T95Nis
T8+CoNis
T9+CoNis
T95+CoNis
T8CoNis
T9CoNis
T95CoNis
Particles
Size (μm)

Figure 6

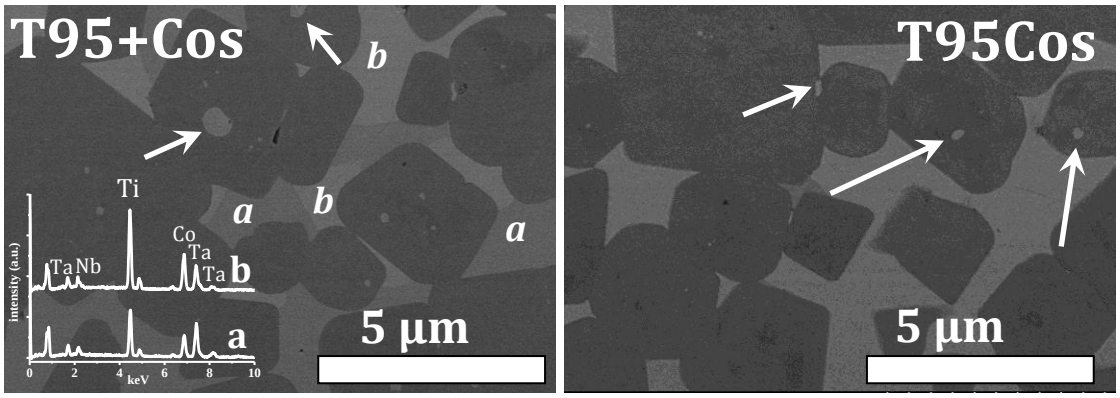
T95+Cos
b
a
b
a
Ti
Co
Ta
Ta
Ta Nb
b
a
intensity (a.u.)
0
2
4
keV
6
8
10
5 µm
T95Cos
5 µm

Figure 7